Antiviral Research 105 (2014) 8–16

Contents lists available at ScienceDirect

Antiviral Research

journal homepage: www.elsevier.com/locate/antiviral

Review

Polymerases of hepatitis C viruses and flaviviruses: Structural and mechanistic insights and drug development

Célia Caillet-Saguy [a], Siew Pheng Lim [b], Pei-Yong Shi [b], Julien Lescar [c,d,*], Stéphane Bressanelli [e,*]

[a] Unité de RMN des Biomolécules, CNRS UMR 3528, Institut Pasteur, 28 rue du Docteur Roux, 75015 Paris, France
[b] Novartis Institute for Tropical Diseases, 10 Biopolis Road, #05-01, Chromos, Singapore 138670, Singapore
[c] School of Biological Sciences, Nanyang Technological University, 60 Nanyang Drive, Singapore 637551, Singapore
[d] INSERM UMRS 945 "Immunité et Infection", Centre Hospitalier Universitaire Pitié-Salpêtrière, Faculté de Médecine et Université Pierre et Marie Curie, 91 Bd de l'Hôpital, 75013 Paris, France
[e] Virologie Moléculaire et Structurale, CNRS UPR3296, 1 Avenue de la Terrasse, 91198 Gif-sur-Yvette Cedex, France

ARTICLE INFO

Article history:
Received 19 December 2013
Revised 31 January 2014
Accepted 10 February 2014
Available online 19 February 2014

Keywords:
Flaviviridae
RNA-dependent RNA polymerase
RNA synthesis
RdRp regulation
Nucleoside inhibitors
Non-nucleoside inhibitors

ABSTRACT

The family *Flaviviridae* comprises several major human pathogens including hepatitis C virus (genus hepacivirus), yellow fever virus, West Nile virus and dengue virus (genus flavivirus). *Flaviviridae* genomes comprise a single-stranded RNA segment encoding a single polyprotein that is subsequently processed into 10 mature viral proteins. The nonstructural proteins are released from the C-terminus of the polyprotein and contribute to the infectious cycle by forming membrane-bound, multi-protein compartments within host cells, named the replication complexes, where synthesis of new viral genomes takes place. Two nonstructural proteins are endowed with multiple enzymatic activities and represent important targets against which specific antiviral inhibitors have been developed. X-ray crystal structures of these viral enzymes as well as in-depth understanding of the molecular basis of their activities have contributed tremendously to the development of antiviral compounds, currently approved or in advanced clinical trials for hepatitis C treatment. One of the prime targets is the RNA-dependent RNA polymerase (RdRp, NS5B for hepatitis C virus, NS5 for flaviviruses). Here we review current knowledge of the structural basis for viral RNA synthesis by NS5B and NS5. These data offer perspectives for further drug design and constitute major advances in our basic understanding of viral RdRp. They thus point to future research directions in the field.

Contents

* Corresponding authors. Addresses: INSERM UMRS 945 "Immunité et Infection", Centre Hospitalier Universitaire Pitié-Salpêtrière, Faculté de Médecine et Université Pierre et Marie Curie, 91 Bd de l'Hôpital, 75013 Paris, France (J. Lescar). Virologie Moléculaire et Structurale, CNRS UPR3296, 1 Avenue de la Terrasse, 91198 Gif-sur-Yvette Cedex, France. Tel.: +33 169823852 (S. Bressanelli).
E-mail addresses: Julien@ntu.edu.sg (J. Lescar), stephane.bressanelli@vms.cnrs-gif.fr (S. Bressanelli).

http://dx.doi.org/10.1016/j.antiviral.2014.02.006
0166-3542/

1. Introduction

The family *Flaviviridae* comprises a large number of viruses which are major public health problems, particularly hepatitis C virus (HCV) in the hepacivirus genus or yellow fever, dengue and Japanese encephalitis viruses in the flavivirus genus (Lindenbach et al., 2007). The pestiviruses make up the third genus in the *Flaviviridae* family and comprise important animal pathogens such as bovine viral diarrhea virus (BVDV). The global incidence of the four serotypes of dengue virus has been on the rise for the last 20 years. Transmitted by the mosquito Aedes aegypti, dengue virus infects an estimated 390 million people annually (Bhatt et al., 2013). Severe forms of dengue fever: dengue haemorrhagic fever (DHF) and dengue shock syndrome (DSS) lead to hospitalization of about 500,000 people each year with an associated mortality of ≈2.5%.

Effective vaccines are available against several flaviviruses including yellow fever, Japanese encephalitis and tick-borne encephalitis viruses (Heinz and Stiasny, 2012). A recombinant, live, attenuated tetravalent dengue vaccine from Sanofi, based on the yellow fever 17D vaccine strain, was recently tested in a large phase IIb clinical trials and failed to confer protection against serotype 2 infection (Sabchareon et al., 2012). Ongoing multi-centred Phase III efficacy studies will shed further light on its effectiveness for pan-serotype protection. On the other hand, despite ongoing research, there is no candidate for preventive or curative vaccines against HCV. An estimated 130–170 million people are chronically infected with HCV which progresses to liver cirrhosis and hepatocellular carcinoma over the course of 20–30 years. Approximately 350,000 people die each year from HCV-related diseases, yet HCV infection is the only chronic viral disease that is curable today (Pawlotsky, 2013).

2. Current treatment

Since the late 1980s, a nonspecific treatment for hepatitis C has been defined by trial and error (Chevaliez and Pawlotsky, 2007). Based on repeated injections of interferon for 24–48 weeks, it was eventually supplemented with ribavirin, a compound that greatly potentiates the effect of interferon. A further important improvement came with pegylation of interferon that enhanced its pharmacokinetic properties. Still, this treatment is fraught with adverse side effects frequently leading to discontinuation. Moreover, on average, treatment leads to a sustained virological response in only about 50% of cases. The response to treatment is dependent on a number of host and viral factors, a major factor being the HCV genotype that infects the patient. Thus, genotype 1, the most prevalent genotype in developed countries, and genotype 4 (that infects up to 15% of people in Egypt) are particularly resistant to pegylated interferon + ribavirin (approximately 40% sustained virological response with the most extensive regimen of up to 72 weeks).

The rate of cure has been greatly improved for genotype 1 (to about 70%) with approval of two protease inhibitors directed against the viral NS3-NS4A protease (Pawlotsky, 2013). These inhibitors are now added to the pegylated interferon + ribavirin treatment, which remained the standard of care for genotypes 2–7 until very recently and is still the standard for genotypes 5–7. New molecules in the pipeline are promising when used in combination indicating that all-oral, interferon-free regimens with very high cure rates can be achieved for HCV in the coming years. These regimens will combine compounds directed against different targets in the HCV replication cycle, such as the viral NS3-4A protease (the "second-wave, first-generation" inhibitors), interaction hub protein NS5A ("second-generation" inhibitors with broad genotype coverage and higher barrier to resistance) and NS5B polymerase (both nucleoside and non-nucleoside inhibitors). Indeed, there has been very recent approval in the USA and Europe of the NS5B-targeted nucleoside analog sofosbuvir for treatment of genotype 1–4 HCV, for now in combination with pegylated interferon and/or ribavirin.

The current treatment for dengue is mostly symptomatic and given when a number of warning signs are observed in association with DHF or DSS. Thus, current treatment includes the administration of pain relievers with acetaminophen (but avoiding those containing ibuprofen, Naproxen or aspirin because of their potential for enhancing hemorrhage), fluid replacement to prevent dehydration, and avoiding mosquito bites to prevent further propagation of the outbreak. In contrast to HCV, which is a chronic infectious disease, infection with dengue virus leads to an acute disease. Studies with dengue patients (with less than 48 h onset of symptoms) revealed that viremia levels decline rapidly in the absence of drug intervention. There is up to 10-fold viremia reduction within 24 h and up to 100-fold within 48 h (Libraty et al., 2002a,b). Thus, a key driver for effective treatment of dengue would be the ability to diagnose the disease early, as reviewed in (Lim et al., 2013a).

3. The *Flaviviridae* replication cycle

The *Flaviviridae* are enveloped viral particles with an outer glycoprotein shell and an inner host-derived lipid bilayer, which surrounds the nucleocapsid comprising the genome RNA and capsid proteins (C). Virus particles first attach to specific host surface receptors, followed by entry into the cell via clathrin-mediated endocytosis (Blanchard et al., 2006; van der Schaar et al., 2008). The genome is subsequently released into the host cell cytoplasm where it is translated into a single polyprotein (Fig. 1).

The single-stranded, positive-sense 9.6–11 kb viral genome acts as messenger RNA for the synthesis of the polyprotein precursor on the endoplasmic reticulum (ER) membrane and induces formation of an ER-derived membranous compartment, where synthesis of new viral genomes takes place (Westaway et al., 1997; Mackenzie et al., 1998; Welsch et al., 2009; Romero-Brey et al., 2012). The single open reading frame is flanked by non-coding sequences that are involved in translation and replication. In flaviviruses such as dengue virus (Fig. 1A), the polyprotein precursor is cleaved by cellular and viral proteases into three structural proteins C, prM and E, and seven non-structural proteins with the enzymatic activities encoded within NS3 and NS5. NS3 has both protease and helicase functions, with NS2B acting as a cofactor for the protease. NS5 comprises both the methyltransferase and polymerase activities. Whilst these enzymatic functions have been extensively characterized, much remains to be learned about their interactions as well as proteins NS1, NS2A, NS4A and NS4B that play equally essential roles in the replication complex.

In hepatitis C virus, polyprotein processing also results in the formation of three structural proteins at its N-terminus and seven nonstructural proteins at its C-terminus. The structural proteins are the capsid protein C and the envelope proteins E1 and E2. The nonstructural proteins are the viroporin p7, the autoprotease NS2, the protease-helicase NS3, the NS3 protease cofactor NS4A (functionally equivalent to NS2B in flaviviruses), the membrane-remodeling NS4B protein (functionally equivalent to NS4A in flaviviruses), the interaction hub NS5A and the polymerase NS5B (Fig. 1B).

A notable difference between the genomes of HCV and flaviviruses is the presence of an internal ribosome entry site in the former, also found in the genome of pestiviruses. In contrast, the flavivirus RNA genome comprises a type 1 cap at its 5′ end and the NS5 protein harbors a methyltransferase domain that is missing in the HCV and pestivirus NS5B proteins. A review on capping

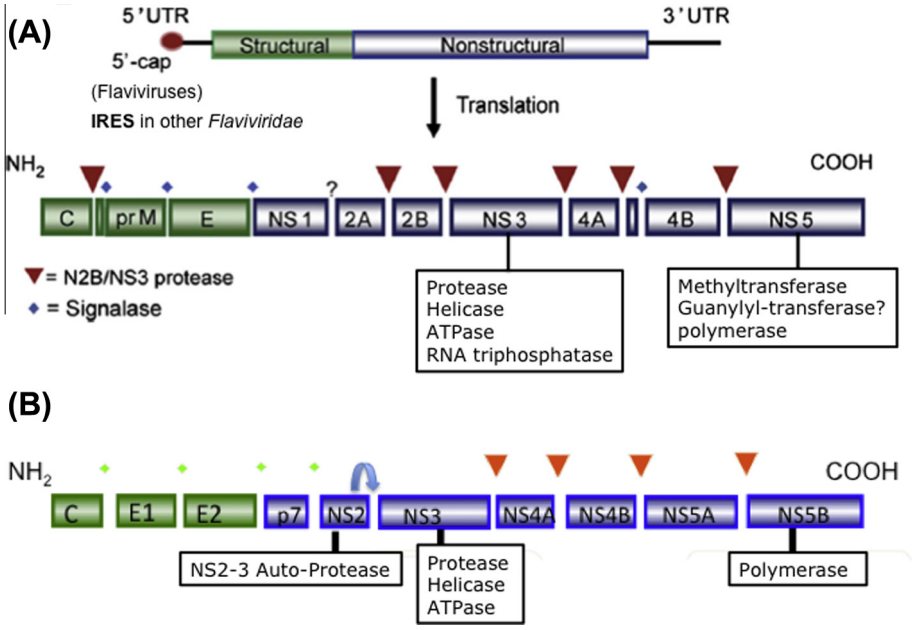

Fig. 1. Translation and proteolytic processing of the *Flaviviridae* polyproteins. The *Flaviviridae* genome is a single-stranded positive-sense RNA molecule. The structural proteins are encoded in the 5′ part and the nonstructural proteins in the 3′ part. In flaviviruses the 11-kb genome comprises a 5′ cap (m7G5′ppp5′A) while the hepaciviruses (9.6 kb) and pestiviruses (12.3 kb) harbor an internal ribosome entry site (IRES). UTR: Untranslated regions. (A) Processing of the flavivirus polyprotein. (B) Processing of the HCV polyprotein. Cleavages by host proteases are indicated by diamonds and cleavages by NS3 are indicated by triangles.

strategies in RNA viruses has been published recently (Decroly et al., 2012). Below, we summarize our current knowledge of the molecular bases of synthesis of new viral RNA by the polymerases of HCV NS5B and flavivirus NS5, with an emphasis on the mechanistic insights and drug design opportunities brought by structural data for these enzymes.

4. The flavivirus polymerase NS5 and the HCV polymerase NS5B

The *Flaviviridae* polymerases are localized to the C-terminal segment of the viral polyprotein and are cleaved by the NS3 protease into the mature polymerase. Flavivirus NS5 is not membrane-anchored and comprises about 900 amino-acids (aa) with its N-terminal ~270 aa bearing a methyltransferase domain (MTase) and its C-terminal ~620 aa encoding polymerase activity. The MTase is involved in type 1 cap synthesis at the 5′ end of the flaviviral genomic RNA. It has at least two activities: guanine N7 methyltransferase and nucleoside 2′-*O* ribose methyltransferase, with a single cofactor-binding site for S-adenosyl-L-methionine (Fig. 2F). Mechanistically, either two NS5 molecules are involved in cap formation assuming a mechanism with one methylation "in trans" (Assenberg et al., 2007; Dong et al., 2008a; Yap et al., 2010), or the RNA substrate must relocate to allow the two successive methylation events to be performed by a single protein (Dong et al., 2008b; Decroly et al., 2012).

In HCV, NS5B comprises 591 aa and is ER-anchored by its C-terminal transmembrane helix (Fig. 2A), with the polymerase domain on the cytosolic side. No MTase domain is found within the HCV NS5B protein, in agreement with a viral RNA translation strategy that involves an internal ribosome entry site for both hepaciviruses and pestiviruses (Lindenbach et al., 2007). Most biochemical studies and all structural studies have been performed with recombinant NS5B proteins devoid of their C-terminal membrane anchor.

For HCV and flaviviruses, a wealth of enzymatic studies has established that NS5B and NS5, respectively, are RNA-dependent RNA polymerases. In the absence of protein cofactors (notably without the NS3 helicase), they require only magnesium or manganese divalent ions to synthesize complementary RNA strands to viral or non-viral RNA templates *in vitro*. This dependence on magnesium (or manganese) is in agreement with the idea that all polynucleotide polymerases (RNA-dependent RNA polymerases, DNA-dependent RNA polymerases (transcriptases), DNA-dependent DNA polymerases (DNA replicases) and RNA-dependent DNA polymerases (reverse transcriptases)) work by the same mechanism (Steitz, 1998). Their roles are to (i) precisely position an incoming nucleotide to base-pair with a single-stranded template and (ii) directly add this nucleotide, in nucleoside monophosphate form, to the 3′ end of the primer strand (Fig. 3C). We refer below to RNA-dependent RNA polymerases as "RdRp" and to single-subunit polymerases as "polymerases".

As soon as the first polymerase structure became available (Ollis et al., 1985), sequence comparisons allowed identification of a number of conserved motifs involved in catalysis, notably in positioning the incoming nucleotide and the catalytic divalent ions (Ollis et al., 1985; Delarue et al., 1990). The HCV-NS5B crystal structure was the first complete RdRp structure (Ago et al., 1999; Bressanelli et al., 1999; Lesburg et al., 1999). It confirmed that the general architecture of polymerases is conserved in viral RdRps. This architecture is likened to a right hand with three subdomains termed, "fingers", "palm" and "thumb" (Fig. 2B).

In the HCV-NS5B structure, three original structural elements were also revealed (Fig. 2C): first, NS5B harbors an extension of the fingers called "fingertips" (Bressanelli et al., 1999) which links the fingers and thumb domains at the back of the RdRp, leaving only a narrow tunnel for the access of incoming nucleotides to the catalytic site. All previous and subsequent work on polymerases, either from model systems (Steitz, 2006) or from important pathogens (Huang et al., 1998), show that in contrast, for non-RdRp polymerases, fingers and thumb move independently of each other on either side of the palm domain. This independence is functionally important: For instance, in non-RdRp polymerases, binding of the incoming nucleotide to the ternary complex of polymerase:template:primer involves a large closure of the fingers while

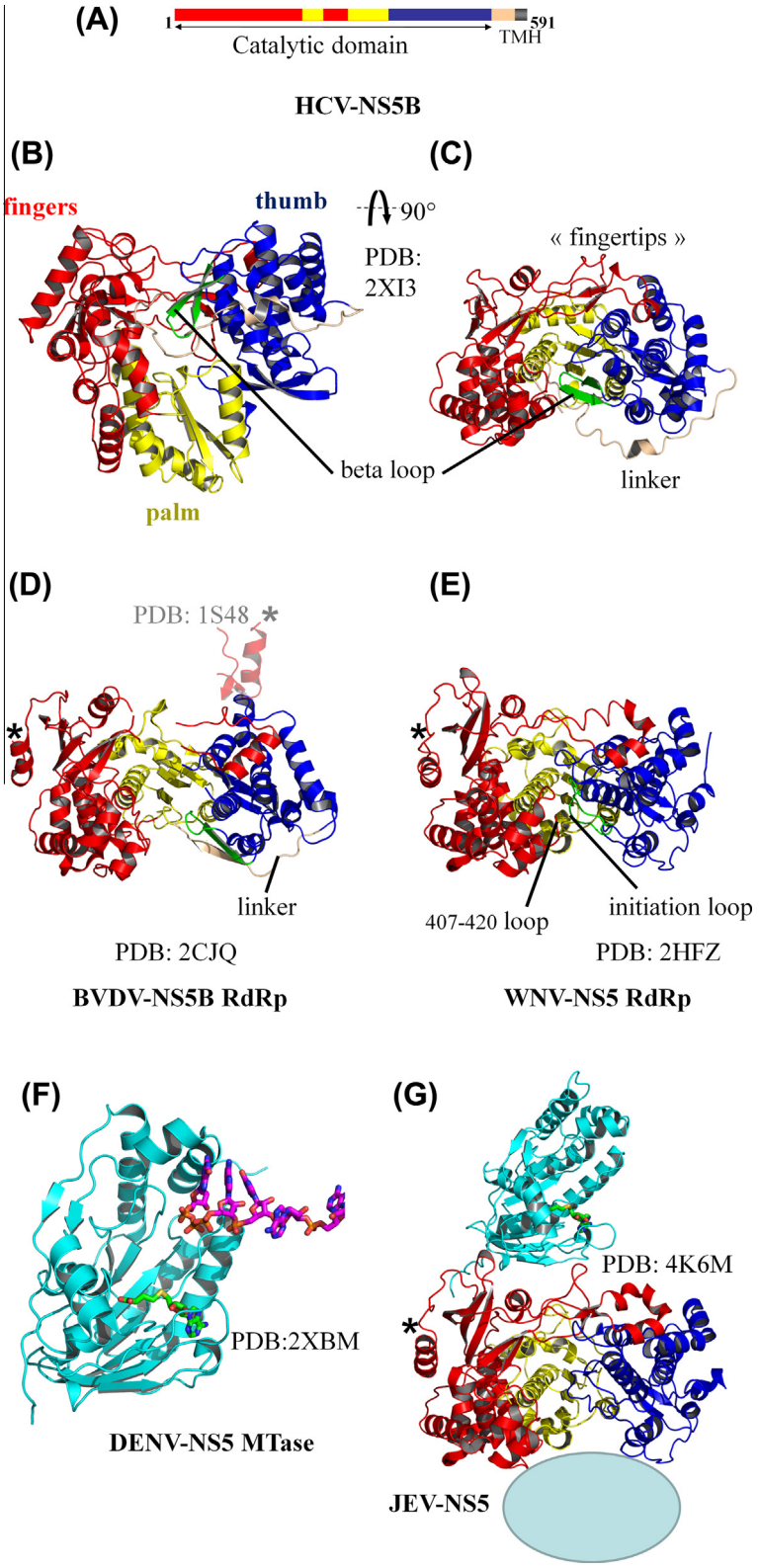

Fig. 2. Atomic structures of *Flaviviridae* NS5B (hepaciviruses, pestiviruses) and NS5 (flaviviruses). In panels (C–E) and (G) structures are displayed to the same scale in the same orientation and colored by the three canonical polymerase subdomains fingers (red), palm (yellow) and thumb (blue). In panels (D), (E) and (G), the asterisks denote the extra elements at the N-terminus of the RdRp domains in the two-domain pestivirus NS5B and flavivirus NS5. (A–C) HCV-NS5B. (A) Primary structure showing its organization as an RdRp domain and transmembrane helix (TMH) connected by a linker segment. (B and C) Two views in ribbon representation at two angles 90° apart, colored by subdomains as in panel (A). The beta-loop that is specific to *Flaviviridae* polymerases is colored green and labeled. (B) Fingers, palm and thumb are labeled. (C) The three key elements discussed in the text fingertips (present in all viral RdRp), linker (present in most *de novo* initiating viral RdRp) and beta-loop are labeled. (D) The pestivirus NS5B RdRp also has a linker and beta-loop, but the latter is shorter than HCV-NS5B's and does not reach down to the active site. The alternate position of the extra N-terminal elements is displayed in semitransparent colors. (E–G) The flavivirus NS5. (E) The RdRp domain of west Nile virus NS5. Note the absence of linker in the flavivirus RdRp. (F) The MTase domain of dengue virus NS5 colored cyan. Displayed as sticks are a short cap-0 RNA (carbons in magenta) and the MTase cofactor (carbons in green) S-adenosyl-L methionine (actually the reaction product S-adenosyl-L homocysteine that co-purifies with recombinant NS5 MTase). (G) The full-length NS5 of Japanese encephalitis virus. The cyan ellipse denotes the approximate position initially proposed for the MTase (Malet et al., 2007).

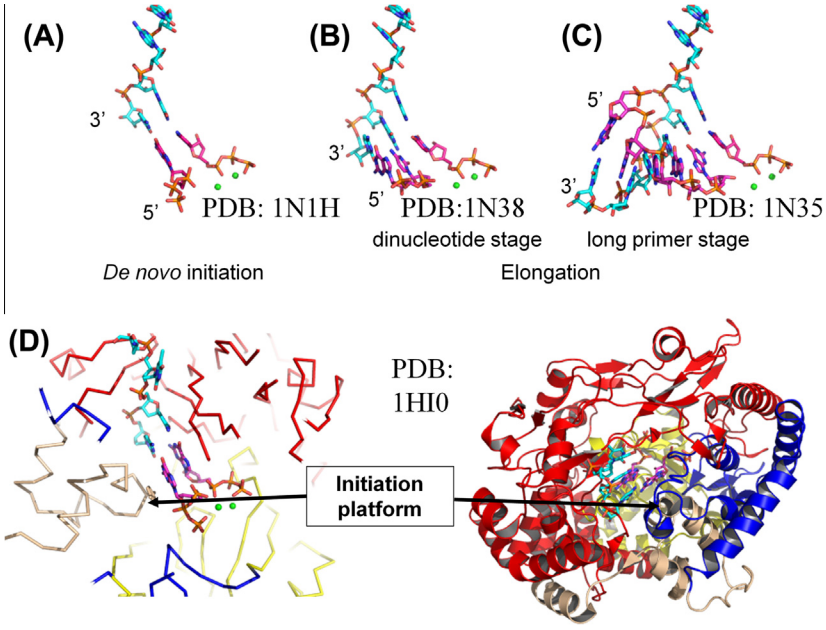

Fig. 3. *De novo* initiation of RNA synthesis captured at atomic resolution for RdRp homologous to NS5B and NS5. (A–C) only the substrates (RNA, nucleotides) and cofactors (two divalent ions in green) are displayed at successive steps of *de novo* synthesis by the reovirus RdRp (Tao et al., 2002). The 3′ end of the template strand and 5′ end of the primer strand (for (A): of the initiating nucleotide) are labeled. (D) Initiation complex of phage φ6 RdRp (Butcher et al., 2001) colored by subdomains as for *Flaviviridae* RdRp. Right, same scale and orientation as in Fig. 2(C–E) and (G). The initiation platform is required to stabilize the base of the initiating nucleotide but must be removed as early as the dinocleotide stage shown in (B).

the thumb mostly keeps its ternary complex conformation. RdRp seem to be a special case as the fingertips have been subsequently found in all structures of viral RdRp (see below). Thus all viral RdRp harbor pre-closed fingers and an NTP tunnel.

A second surprise of the HCV-NS5B structure was a "beta-loop" (or "beta-flap") inserted in the thumb and projecting towards the active site. This beta-loop (colored in green on Fig. 2B and C), also called "initiation" or "priming-loop", as well as the closure and bulk of the thumb would prevent egress of the 5′ end of the primer RNA strand in models of the ternary polymerase:template:primer elongation complex. The beta-loop is also present in the flavivirus NS5 (Malet et al., 2007; Yap et al., 2007) (Fig. 2E) and in the pestivirus NS5B (Choi et al., 2004) (Fig. 2D), but not in other viral RdRp of known structure. For instance, it is missing in all structures of *Picornaviridae* RdRp, that have much smaller thumb domains. It is thus a signature of the *Flaviviridae* RdRp (Lescar and Canard, 2009).

Finally, the third surprise in the HCV-NS5B structure was the positioning of some 40 residues downstream of the polymerase domain that connect this domain to the transmembrane anchor *in vivo* and which for this reason we term "linker" (Fig. 2C). In HCV-NS5B, this linker is always organized as a long loop around the thumb that obstructs the front part of NS5B (Caillet-Saguy et al., 2011) by establishing specific contacts with the beta loop (Adachi et al., 2002). In this location, the linker prevents egress of the 3′ end of the template RNA strand and also contributes to keeping the thumb in a closed conformation (Caillet-Saguy et al., 2011) (Harrus et al., 2010).

5. The central issue of RNA synthesis initiation in *Flaviviridae*

Several viral RdRp display a peculiar mode of initiation of RNA synthesis: They start RNA synthesis from the 3′ end of a template strand without any primer. This so-called '*de novo*' synthesis involves the initial condensation of two nucleotides complementary to the two 3′-terminal bases of the single-stranded RNA template (Fig. 3A). With the exception of the flavivirus NS5, all viral RdRp with *de novo* initiation capability harbor a C-terminal extension to the polymerase domain that folds back towards the catalytic site. In contrast, RdRp that perform only primer extension, such as the picornavirus RdRp, do not have C-terminal extensions, display an open catalytic site and can bind double-stranded template:primer RNA with only minor conformational adjustments (Ferrer-Orta et al., 2009). A striking case in this respect is the *Caliciviridae* RdRp of which structures are available for noroviruses and sapoviruses. This RdRp can perform both protein-primed and *de novo* RNA synthesis (Rohayem et al., 2006). Structurally, the calicivirus RdRp is most similar to the picornavirus RdRp that performs only protein-primed RNA synthesis. However, unlike the picornavirus RdRp, the calicivirus RdRp harbors a short C-terminal extension at the exit from the catalytic site, which is displaced in the elongation phase (Zamyatkin et al., 2008).

The capability for *de novo* RNA synthesis has been established *in vitro* for NS5B (Oh et al., 1999) and NS5 (Ackermann and Padmanabhan, 2001) and this mechanism is now assumed for all *Flaviviridae in vivo*. It is known that RdRp from double-stranded RNA viruses are homologous to those of single-stranded, positive-sense RNA viruses like *Flaviviridae* (Gorbalenya and Koonin, 1988). Seminal structural data of RdRp from double-stranded RNA reovirus and φ6 phage (that also initiate RNA synthesis *de novo*) have provided a molecular framework for this phenomenon (Butcher et al., 2001; Tao et al., 2002). These works highlighted the involvement of a mobile protein initiation platform that stabilizes the base of the initiating nucleotide (Fig. 3D). It then moves out of the way to allow elongation of the first, dinucleotide primer. In reovirus RdRp, the platform is a short insertion in the palm subdomain (Tao et al., 2002). In contrast, in the φ6 RdRp the C-terminal extension harbors the tyrosine that makes up the initiation platform (Butcher et al., 2001) (Fig. 3D), as well as a specific recognition pocket for the 3′ end of the template.

No structure of an initiation complex is available for a *Flaviviridae* RdRp, so it is not known which region of the protein provides

the initiation platform. For HCV-NS5B, a conserved tyrosine at the tip of the beta-loop that is engaged in a network of interactions with palm and linker (Adachi et al., 2002) is spatially close to the expected position for the initiation platform (Harrus et al., 2010). However, in the pestivirus NS5B (Fig. 2D), the beta-loop is shorter and its tip too far from the palm to provide the initiation platform. The BVDV NS5B binds a GTP next to the expected site of the initiation nucleotide and this extra GTP could provide the initiation platform (Choi et al., 2004).

The case of the flavivirus NS5 is a complex one for at least two reasons. First, the NS5 N-terminal methyltransferase domain is involved in synthesis of the type 1 cap at the 5′ end of the flavivirus genomic RNA. It is likely that cap addition occurs almost simultaneously with initiation of positive strand synthesis. It has been proposed that the MTase domain is positioned at the RNA exit channel from the RdRp domain and binds the newly synthesized 5′ end of the positive strand (Malet et al., 2007). However, an important recent structure of the full length NS5 protein from JEV (Lu and Gong, 2013) unexpectedly locates the MTase on the other side of the RdRp, in contact with the base of the fingertips (Fig. 2G). Residues lining the base of the MTase active site thus interact with residues overhanging the NTP entry channel. This interface is conserved in flaviviruses, suggesting that it is relevant to replication. It may modulate NS5's fingertips flexing during RNA synthesis. Still, for 5′ RNA cap methylation to occur in the expected manner, the MTase domain would need to translocate to the RNA exit channel of RdRp (Fig. 2G).

Alternately, the 5′ cap of the nascent RNA could be directed back to the MTase active site and/or be methylated by two NS5 molecules. Indeed, a functional oligomerization of MTase was proposed based on crystallographic structures of MTase in complex with cap analogues (Assenberg et al., 2007). In this model, the two S-adenosyl-L-methionine cofactors on either side of an MTase dimeric interface would provide the two methyl groups for successive modification of the cap's adenosine N7 and ribose 2′-OH. Additional crystal structures with 5′-capped RNA octamers also support the view that NS5 may perform its cap-related functions in an oligomeric form (Yap et al., 2010). This is corroborated by a dimeric RdRp structure obtained with an N-terminally extended RdRp construct bearing residues from the NS5 interdomain linker. Based on this and the JEV full-length NS5 structure, residues 263–267 are believed to provide the necessary flexibility for the two domains to perform their respective functions (Lu and Gong, 2013; Lim et al., 2013b). In relation to this possible flexibility in the connection between the two domains, it is useful to compare NS5 to the pestivirus NS5B that also harbors an extra domain (of unknown function) of some 90 residues N-terminal to the polymerase domain. Strikingly, both the pestivirus NS5B and flavivirus NS5 comprise the same extra elements (including a helix labeled by an asterisk on Fig. 2D, E and G) between the core RdRp domain and the extra N-terminal domain. These elements are found in alternate positions in the different crystal structures of BVDV NS5B (Fig. 2D), indicating considerable flexibility at least in the absence of the first 70 residues (Choi et al., 2004, 2006), but are in the same position in NS5 across flavivirus species and constructs (Fig. 2E and G).

A second feature points to the specificity of the flavivirus NS5: it is the only *de novo* initiating RdRp of known structure devoid of any C-terminal extension (Fig. 2E). Still, the exit from the catalytic site is almost as congested in the NS5 RdRp domain as in other *Flaviviridae* RdRp. This is partly due to the larger protrusion made up by the "initiation loop" (corresponding to the NS5B beta-loop) from the thumb as well as an insertion in the fingers (aa 407–420) that is flexible and may come in contact with the initiation loop (Malet et al., 2007). This interaction brings the tip of the initiation loop in close proximity to the expected position of the initiation platform, similarly to the network of interactions of the beta-loop with the linker and palm domain in HCV-NS5B. Recent work on NS5 has confirmed the involvement of the tip of the initiation loop in *de novo* initiation (Selisko et al., 2012). The central residue does not seem to be the conserved tryptophan as initially proposed (Malet et al., 2007; Yap et al., 2007), but a histidine (His798) three residues downstream in the loop (Selisko et al., 2012).

Regardless of the precise means by which *Flaviviridae* RdRp stabilize their initiation complexes, the next step after the first dinucleotide synthesis must consist in a sequence of large conformational changes. These feature the withdrawal of the initiation platform, allowing egress of the duplex RNA formed by the 5′ end of the primer and the 3′ end of the template strands. In the case of HCV-NS5B, it was postulated that these conformational changes involve both withdrawal of the linker and beta-loop and opening of the thumb in a transition step leading to the formation of a processive elongation complex (Bressanelli et al., 1999; Harrus et al., 2010). The structure of just such a complex was recently published (Mosley et al., 2012) (Fig. 4B). The strategy to obtain this complex was based on the use of an HCV RdRp with extraordinary *de novo* RNA synthesis efficiency, the JFH1 strain NS5B (Simister et al., 2009). The JFH1-NS5B protein is able to both synthesize the first dinucleotide primer and convert to the elongation phase much more proficiently than other HCV NS5B proteins (Scrima et al., 2012).

Furthermore, Mosley et al. (2012) deleted the beta-loop to facilitate RNA-primer-template binding in an open, elongation-like conformation. Not only does this new structure (Fig. 4B) confirm previous postulates but it also brings to light unexpected rearrangements occurring in HCV-NS5B during the transition: The predicted large opening of the thumb (in blue on Fig. 4) indeed occurs, together with a flexing of the fingertips (shown in magenta, at the back of NS5B) and a withdrawal of the linker that becomes largely disordered in the crystal. However, another, unexpected structural change occurs in a loop of the thumb domain (residues 402–406). The loop's residue 405 may be a valine or an isoleucine and this polymorphism modulates efficiency in both *de novo* initiation (Schmitt et al., 2011) and transition to elongation (Scrima et al., 2012). Residues 404–406 (in cyan on Fig. 4) bridge the thumb and fingers and contribute to keeping HCV-NS5B in the closed, initiation-competent conformation (Fig. 4A). This is reminiscent of what is observed in available structures of the flavivirus NS5 RdRp. Indeed

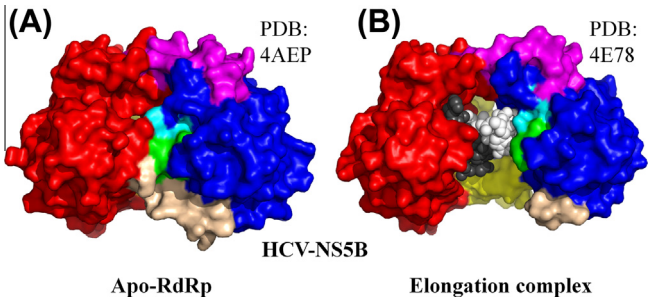

Fig. 4. Conformational changes of HCV-NS5B in the transition from initiation to elongation. Views of the enzyme's molecular surface in the orientation of Fig. 2C (A) before binding the single-stranded RNA template and (B) after binding a template/primer RNA duplex (in black/white). (A) HCV-NS5B is initially in a conformation in which the thumb (in blue) is closed. A loop at the thumb's top (in cyan) stabilizes this closed conformation by crossing the gap to the fingers (in red) and by interacting with the beta-loop (in green). (B) In the elongation complex, the cyan loop has refolded and flipped towards the fingertips (in magenta). The thumb and linker have moved away from the catalytic site. Thus the reoriented and remolded inner surface of the thumb provides a guide for the primer strand instead of occluding the egress for the double-stranded RNA as in (A).

the insertion in NS5 fingers subdomain (residues 407–420) opposite the initiation loop (see above) overlaps with the region of the HCV-NS5B fingers that contacts the 402–406 loop. In the HCV-NS5B elongation complex, the 402–406 loop retracts against the thumb and refolds to contact the flexed fingertips. Altogether, these conformational changes induce the formation of a groove along the opened thumb that guides the exit of the newly synthesized RNA (colored in white on Fig. 4B).

6. Nucleoside and non-nucleoside HCV-NS5B inhibitors in the light of available structural data

The structure of the HCV-NS5B elongation complex certainly heralds new developments in structure-based drug discovery against the *Flaviviridae* RdRp. It may guide attempts for obtaining similar structures of other *Flaviviridae* RdRp bound to RNA. Similar strategies can also be employed to obtain atomic-level views of the action of nucleotide inhibitors (NI) against HCV-NS5B (Mosley et al., 2012). Thus far, only structures of complexes with non-nucleoside inhibitors (NNI) have been published for HCV-NS5B. Screening campaigns in cell culture systems have identified at least four NNI-binding pockets that are currently targeted in clinical trials (Fig. 5A). In contrast, a single pocket of the HIV-1 reverse transcriptase is targeted by NNIs (Yang et al., 2012). It is all the more remarkable that NNI targeting the four HCV-NS5B sites inhibit pre-elongation stages of RNA synthesis, and at least three of them likely by the same mechanism (Caillet-Saguy et al., 2011).

While NNI will certainly be used in future anti-HCV multi-therapies, NI are particularly promising as they have shown stronger antiviral activity, are pan-genotype inhibitory, and have a higher barrier against the emergence of drug-resistance (Pawlotsky, 2013). For instance, the template binding groove involves more than 15 residues including 14-139-160-162 in the fingertips, 93-95-96-97-168-172-180 in the fingers and 282-283-284-285 in the connection between fingers and palm, yet among those only conservative mutations at positions 96 and 282 have been selected in cell culture under NI treatment. Indeed, when mapped onto the structure of the HCV-NS5B elongation complex, resistance mutations to NI display an interesting pattern (Fig. 5B). Only S282T is in a position to directly interfere with an NI at the catalytic site. This suggests the existence of several mechanisms inducing resistance to NI for HCV-NS5B. For instance, two mutations were consistently reported under 4′-azido nucleotide pressure that should lead to an alteration of the template-primer translocation: S96T located at the entry of the template binding groove inserts between two phosphates of the primer backbone; N142T lies at the hinge point in the fingertips (Caillet-Saguy et al., 2011). Altering translocation after NI incorporation would facilitate excision either by pyrophosphorolysis or by the recently described NTP-mediated nucleotide excision activity of HCV-NS5B (Jin et al., 2013).

Still other resistance mechanisms seem to be at work in the loop overhanging the NTP tunnel, as shown by the P156L and G152E mutations arising under dihydroxypyrimidine pressure. There too, a direct interference with catalysis seems unlikely and resistance may arise by disfavoring entry of NI into the NTP tunnel (Bressanelli et al., 2002). Finally, under pressure from some guanosine analogues, mutations appear in the RdRp C-terminal region. The mutation P540T in the linker may point to a mechanism of resistance affecting a pre-elongation stage, suggesting that this class of NI could even have an NNI-like mechanism of action.

7. Nucleoside and non-nucleoside DENV-NS5 inhibitors in the light of the available structural data

NIs have been reported to inhibit different viral serotypes/genotypes of DENV as well as related viruses. The adenosine analogues NITD008 (beta-D-2′-432 ethynyl-7-deaza-adenosine triphosphate) and NITD203 (3′,5′-*O*-diisobutyryl-2′-*C*-acetylene-7-deaza-433 7-carbamoyladenosine) have EC50s of <1 μM for all four serotypes of DENV and also inhibit related viruses like YFV, WNV and HCV. Both compounds showed *in vivo* efficacy in the DENV-2 AG-129 mouse model. However, neither NI could reach a satisfactory no-observable adverse-effect level (NOAEL) in 2-week *in vivo* toxicity studies in rats and dogs (Yin et al., 2009; Chen et al., 2010). No resistant virus could be recovered from DENV or WNV infected cells after continuous culturing in presence of various compound concentrations for up to 4 months. Thus it is difficult to draw any conclusions about mutational hotspots in the flavivirus RdRp in the presence of these inhibitors.

Recently, an anti-HCV NI, balapiravir, a tri-isobutyrate ester prodrug of 4′-azidocytidine (R1479; (Nelson et al., 2012)) was tested on DENV patients in a phase II clinical trial (Nguyen et al., 2013). Surprisingly, treatment did not influence the clinical and virological parameters in patients, such as the blood viral levels, NS1 production, as well as fever duration. The reason for the lack of efficacy remains to be determined. *In vitro*, balapiravir inhibited DENV replication with EC_{50} values ranging from 1.9–11 μM, 1.3–3.2 μM and 0.103 μM in DENV HuH7 replicon, primary human macrophage (Nguyen et al., 2013) and human peripheral blood mononuclear cells (Chen et al., 2014), respectively. Plasma drug levels in DENV patients dosed with 1500 mg and 3000 mg R1749, twice a day, attained median C_{min} values of 3.56 and 5.8 μM, respectively. It is possible that a higher plasma level of the drug is needed to achieve antiviral effects or the intracellular conversion of the prodrug may not have been optimal. Indeed, Chen et al. observed that pre-infection of DENV-2 in human PBMCs depotentiat-

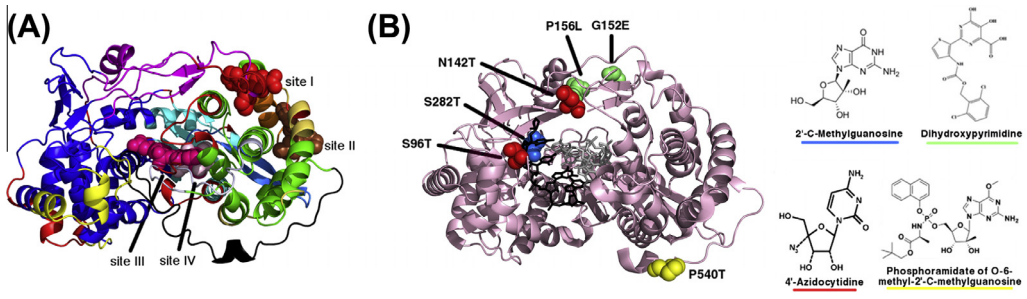

Fig. 5. Non-nucleoside and nucleoside inhibitors in relation to the HCV-NS5B structure. (A): The four distinct NNI binding sites identified by X-ray crystallography and acting at a pre-elongation step. Here the closed thumb conformation is colored by subregions moving as rigid blocks upon NNI binding (Caillet-Saguy et al., 2011). (B): Locations on the elongation complex of mutations appearing in cell culture upon NI pressure. For each of four classes of NI compounds (shown on the right and underlined in colors), the locations of resistance mutations are displayed as spheres and colored by the respective compound they confer resistance to. Note that only residues 282 and 96 are in position to directly interfere with the replicating RNA.

ed the EC_{50} value to 12.85 μM (>100-fold loss in potency from the immediate treatment EC_{50} value of 0.103 μM), which is above the median patient plasma C_{min} of the two doses administered (Chen et al., 2014). The EC_{50} derived from the delayed drug treatment should be more reflective of the therapeutic condition. Of note, no balapiravir-resistant HCV variants were isolated from HCV patients when dosed up to 28 days.

No NNI allosteric sites have been identified in flavivirus RdRp. Surface shape analysis using *in silico* algorithms identified two cavities (A and B) common in the thumb domain of DENV and WNV RdRp and an additional three cavities in WNV. Mutational analyses of conserved residues in these cavities carried out in DENV showed that those in cavity B, but not A, are critical for virus replication and mostly impaired NS5 polymerase activity *in vitro* (Zou et al., 2011). It remains to be seen if cavity B could be used as a starting point for structure-based drug design or for virtual screening. The three cavities in WNV RdRp, located in the thumb and in the fingers subdomains have yet to be characterized.

The Novartis Institute for Tropical Diseases conducted two high-throughput screening (HTS) campaigns (both screened about 1.8 million compounds) using biochemical assays that measured DENV polymerase elongation activities. The first HTS performed with a radioactive scintillation proximity assay identified one compound class that bound at the entrance of the RNA tunnel of the RdRp and likely functions by blocking RNA synthesis. Although submicromolar inhibitory activities were obtained, the series could not be advanced due to lack of a good cellular activity (Yin et al., 2009; Niyomrattanakit et al., 2010). In the second HTS campaign in which a fluorescent coupled assay was used, few specific inhibitors were obtained. One inhibitor, NITD-107 binds to the RdRp as a dimer and causes conformational changes in the protein. Although NITD-107 binds to the DENV RdRp active site, it showed only weak inhibitory activity *in vitro* and no cellular activity (Noble et al., 2013).

8. Concluding remarks

The fact that NNI and possibly some NI target the initiation stage for HCV NS5B points to the great importance of strict regulation of RNA synthesis in HCV, and likewise in all *Flaviviridae*. Indeed, the common *Flaviviridae* strategy of a single polyprotein for genome expression implies overproduction of the RdRp. It must subsequently be tightly regulated at the level of initiation of RNA synthesis. In all known single-stranded, positive-sense RNA viruses, synthesis of new genomes occurs within specific membrane compartments through the activities of a few key viral enzymes. Among single-stranded, positive-sense RNA viruses, *Flaviviridae* have been the subject of many studies because of their high importance in human and animal health. These studies have come to fruition and our understanding of the molecular mechanisms underlying replication of the viral genomes has become more precise and complete. This understanding has contributed powerfully to the development of new antiviral compounds.

The case of HCV is particularly telling. Despite major difficulties in the study of this virus, sustained efforts have led to major advances (Bartenschlager et al., 2013) that have considerable implications for *Flaviviridae* and other single-stranded, positive-sense RNA viruses biology. In this respect, work aiming at deciphering the composition and architecture of *Flaviviridae* replication complexes (Welsch et al., 2009; Romero-Brey et al., 2012) provide unique information not only for basic virology, but also for the design of future therapies. Similarly, one subject of future research on *Flaviviridae* should be a basic issue in single-stranded positive-sense RNA virus replication: the regulation of RdRp (in)fidelity. Indeed, not only must viral RNA be synthesized at the right time and place, but quasispecies diversity must be maintained in the infected host. Thus, the RdRp error rate is finely tuned and it may easily be reduced (Vignuzzi et al., 2006) but at a considerable cost in replicative capacity (Vignuzzi et al., 2008). This issue is of central importance for antiviral intervention targeting RdRp as it may determine whether mutants capable of better discrimination against nucleotide inhibitors will actually be selected in real-life cases. Recent reports of specific fidelity mechanisms in HCV NS5B (Jin et al., 2013) and flavivirus NS5 (Selisko et al., 2012) indicate that atomic level structural studies establishing the molecular basis of these phenomena are now needed.

Acknowledgements

Célia Caillet-Saguy is a recipient of a "Bourse Roux" postdoctoral fellowship from the Pasteur Institute. Stéphane Bressanelli's lab is supported by CNRS and by the French National Agency for Research on AIDS and Viral Hepatitis (ANRS). Julien Lescar's lab was supported by BMRC grant 0912219/599 and partially by CRP grant CRP2008 from the NRF. The authors apologize to all colleagues whose work could not be cited owing to space limitations.

References

Ackermann, M., Padmanabhan, R., 2001. De novo synthesis of RNA by the dengue virus RNA-dependent RNA polymerase exhibits temperature dependence at the initiation but not elongation phase. J. Biol. Chem. 276, 39926–39937.
Adachi, T., Ago, H., Habuka, N., Okuda, K., Komatsu, M., Ikeda, S., Yatsunami, K., 2002. The essential role of C-terminal residues in regulating the activity of hepatitis C virus RNA-dependent RNA polymerase. Biochim. Biophys. Acta 1601, 38–48.
Ago, H., Adachi, T., Yoshida, A., Yamamoto, M., Habuka, N., Yatsunami, K., Miyano, M., 1999. Crystal structure of the RNA-dependent RNA polymerase of hepatitis C virus. Structure 7, 1417–1426.
Assenberg, R., Ren, J., Verma, A., Walter, T.S., Alderton, D., Hurrelbrink, R.J., Fuller, S.D., Bressanelli, S., Owens, R.J., Stuart, D.I., Grimes, J.M., 2007. Crystal structure of the Murray Valley encephalitis virus NS5 methyltransferase domain in complex with cap analogues. J. Gen. Virol 88, 2228–2236.
Bartenschlager, R., Lohmann, V., Penin, F., 2013. The molecular and structural basis of advanced antiviral therapy for hepatitis C virus infection. Nat. Rev. Microbiol. 11, 482–496.
Bhatt, S., Gething, P.W., Brady, O.J., Messina, J.P., Farlow, A.W., Moyes, C.L., Drake, J.M., Brownstein, J.S., Hoen, A.G., Sankoh, O., Myers, M.F., George, D.B., Jaenisch, T., Wint, G.R.W., Simmons, C.P., Scott, T.W., Farrar, J.J., Hay, S.I., 2013. The global distribution and burden of dengue. Nature 496, 504–507.
Blanchard, E., Belouzard, S., Goueslain, L., Wakita, T., Dubuisson, J., Wychowski, C., Rouillé, Y., 2006. Hepatitis C virus entry depends on clathrin-mediated endocytosis. J. Virol. 80, 6964–6972.
Bressanelli, S., Tomei, L., Roussel, A., Incitti, I., Vitale, R.L., Mathieu, M., De Francesco, R., Rey, F.A., 1999. Crystal structure of the RNA-dependent RNA polymerase of hepatitis C virus. Proc. Natl. Acad. Sci. U.S.A. 96, 13034–13039.
Bressanelli, S., Tomei, L., Rey, F.A., De Francesco, R., 2002. Structural analysis of the hepatitis C virus RNA polymerase in complex with ribonucleotides. J. Virol. 76, 3482–3492.
Butcher, S.J., Grimes, J.M., Makeyev, E.V., Bamford, D.H., Stuart, D.I., 2001. A mechanism for initiating RNA-dependent RNA polymerization. Nature 410, 235–240.
Caillet-Saguy, C., Simister, P.C., Bressanelli, S., 2011. An objective assessment of conformational variability in complexes of hepatitis C virus polymerase with non-nucleoside inhibitors. J. Mol. Biol. 414, 370–384.
Chen, Y.-L., Yin, Z., Lakshminarayana, S.B., Qing, M., Schul, W., Duraiswamy, J., Kondreddi, R.R., Goh, A., Xu, H.Y., Yip, A., Liu, B., Weaver, M., Dartois, V., Keller, T.H., Shi, P.-Y., 2010. Inhibition of dengue virus by an ester prodrug of an adenosine analog. Antimicrob. Agents Chemother. 54, 3255–3261.
Chen, Y.-L., Abdul Ghafar, N., Karuna, R., Fu, Y., Lim, S.P., Schul, W., Gu, F., Herve, M., Yokohama, F., Wang, G., Cerny, D., Fink, K., Blasco, F., Shi, P.-Y., 2014. Activation of peripheral blood mononuclear cells by dengue virus infection depotentiates balapiravir. J. Virol. 88, 1740–1747.
Chevaliez, S., Pawlotsky, J.-M., 2007. Interferon-based therapy of hepatitis C. Adv. Drug Delivery Rev 59, 1222–1241.
Choi, K.H., Groarke, J.M., Young, D.C., Kuhn, R.J., Smith, J.L., Pevear, D.C., Rossmann, M.G., 2004. The structure of the RNA-dependent RNA polymerase from bovine viral diarrhea virus establishes the role of GTP in de novo initiation. Proc. Natl. Acad. Sci. U.S.A. 101, 4425–4430.
Choi, K.H., Gallei, A., Becher, P., Rossmann, M.G., 2006. The structure of bovine viral diarrhea virus RNA-dependent RNA polymerase and its amino-terminal domain. Structure 14, 1107–1113.
Decroly, E., Ferron, F., Lescar, J., Canard, B., 2012. Conventional and unconventional mechanisms for capping viral mRNA. Nat. Rev. Microbiol. 10, 51–65.

Delarue, M., Poch, O., Tordo, N., Moras, D., Argos, P., 1990. An attempt to unify the structure of polymerases. Protein Eng. 3, 461–467.
Dong, H., Ren, S., Li, H., Shi, P.-Y., 2008a. Separate molecules of West Nile virus methyltransferase can independently catalyze the N7 and 2′-O methylations of viral RNA cap. Virology 377, 1–6.
Dong, H., Ren, S., Zhang, B., Zhou, Y., Puig-Basagoiti, F., Li, H., Shi, P.-Y., 2008b. West Nile virus methyltransferase catalyzes two methylations of the viral RNA cap through a substrate-repositioning mechanism. J. Virol. 82, 4295–4307.
Ferrer-Orta, C., Agudo, R., Domingo, E., Verdaguer, N., 2009. Structural insights into replication initiation and elongation processes by the FMDV RNA-dependent RNA polymerase. Curr. Opin. Struct. Biol. 19, 752–758.
Gorbalenya, A.E., Koonin, E.V., 1988. Birnavirus RNA polymerase is related to polymerases of positive strand RNA viruses. Nucleic Acids Res. 16, 7735.
Harrus, D., Ahmed-El-Sayed, N., Simister, P.C., Miller, S., Triconnet, M., Hagedorn, C.H., Mahias, K., Rey, F.A., Astier-Gin, T., Bressanelli, S., 2010. Further insights into the roles of GTP and the C terminus of the hepatitis C virus polymerase in the initiation of RNA synthesis. J. Biol. Chem. 285, 32906–32918.
Heinz, F.X., Stiasny, K., 2012. Flaviviruses and flavivirus vaccines. Vaccine 30, 4301–4306.
Huang, H., Chopra, R., Verdine, G.L., Harrison, S.C., 1998. Structure of a covalently trapped catalytic complex of HIV-1 reverse transcriptase: implications for drug resistance. Science 282, 1669–1675.
Jin, Z., Leveque, V., Ma, H., Johnson, K.A., Klumpp, K., 2013. NTP-mediated nucleotide excision activity of hepatitis C virus RNA-dependent RNA polymerase. Proc. Natl. Acad. Sci. U.S.A. 110, E348–E357.
Lesburg, C.A., Cable, M.B., Ferrari, E., Hong, Z., Mannarino, A.F., Weber, P.C., 1999. Crystal structure of the RNA-dependent RNA polymerase from hepatitis C virus reveals a fully encircled active site. Nat. Struct. Biol 6, 937–943.
Lescar, J., Canard, B., 2009. RNA-dependent RNA polymerases from flaviviruses and Picornaviridae. Curr. Opin. Struct. Biol. 19, 759–767.
Libraty, D.H., Endy, T.P., Houng, H.-S.H., Green, S., Kalayanarooj, S., Suntayakorn, S., Chansiriwongs, W., Vaughn, D.W., Nisalak, A., Ennis, F.A., Rothman, A.L., 2002a. Differing influences of virus burden and immune activation on disease severity in secondary dengue-3 virus infections. J. Infect. Dis. 185, 1213–1221.
Libraty, D.H., Young, P.R., Pickering, D., Endy, T.P., Kalayanarooj, S., Green, S., Vaughn, D.W., Nisalak, A., Ennis, F.A., Rothman, A.L., 2002b. High circulating levels of the dengue virus nonstructural protein NS1 early in dengue illness correlate with the development of dengue hemorrhagic fever. J. Infect. Dis. 186, 1165–1168.
Lim, S.P., Wang, Q.-Y., Noble, C.G., Chen, Y.-L., Dong, H., Zou, B., Yokokawa, F., Nilar, S., Smith, P., Beer, D., Lescar, J., Shi, P.-Y., 2013a. Ten years of dengue drug discovery: progress and prospects. Antiviral Res. 100, 500–519.
Lim, S.P., Koh, J.H.K., Seh, C.C., Liew, C.W., Davidson, A.D., Chua, L.S., Chandrasekaran, R., Cornvik, T.C., Shi, P.-Y., Lescar, J., 2013b. A crystal structure of the dengue virus non-structural protein 5 (NS5) polymerase delineates interdomain amino acid residues that enhance its thermostability and de novo initiation activities. J. Biol. Chem. 288, 31105–31114.
Lindenbach, B.D., Thiel, H.J., Rice, C.M., 2007. Flaviviridae: the viruses and their replication. In: Knipe, D.M., Howley, P.M. (Eds.), Fields Virology. Lippincott-Raven Publishers, Philadelphia, pp. 1101–1152.
Lu, G., Gong, P., 2013. Crystal structure of the full-length Japanese encephalitis virus NS5 reveals a conserved methyltransferase-polymerase interface. PLoS Pathog. 9, e1003549.
Mackenzie, J.M., Khromykh, A.A., Jones, M.K., Westaway, E.G., 1998. Subcellular localization and some biochemical properties of the flavivirus Kunjin nonstructural proteins NS2A and NS4A. Virology 245, 203–215.
Malet, H., Egloff, M.-P., Selisko, B., Butcher, R.E., Wright, P.J., Roberts, M., Gruez, A., Sulzenbacher, G., Vonrhein, C., Bricogne, G., Mackenzie, J.M., Khromykh, A.A., Davidson, A.D., Canard, B., 2007. Crystal structure of the RNA polymerase domain of the West Nile virus non-structural protein 5. J. Biol. Chem. 282, 10678–10689.
Mosley, R.T., Edwards, T.E., Murakami, E., Lam, A.M., Grice, R.L., Du, J., Sofia, M.J., Furman, P.A., Otto, M.J., 2012. Structure of hepatitis C virus polymerase in complex with primer-template RNA. J. Virol. 86, 6503–6511.
Nelson, D.R., Zeuzem, S., Andreone, P., Ferenci, P., Herring, R., Jensen, D.M., Marcellin, P., Pockros, P.J., Rodríguez-Torres, M., Rossaro, L., Rustgi, V.K., Sepe, T., Sulkowski, M., Thomason, I.R., Yoshida, E.M., Chan, A., Hill, G., 2012. Balapiravir plus peginterferon alfa-2a (40KD)/ribavirin in a randomized trial of hepatitis C genotype 1 patients. Ann. Hepatol. 11, 15–31.
Nguyen, N.M., Tran, C.N.B., Phung, L.K., Duong, K.T.H., Huynh Hle, A., Farrar, J., Nguyen, Q.T.H., Tran, H.T., Nguyen, C.V.V., Merson, L., Hoang, L.T., Hibberd, M.L., Aw, P.P.K., Wilm, A., Nagarajan, N., Nguyen, D.T., Pham, M.P., Nguyen, T.T., Javanbakht, H., Klumpp, K., Hammond, J., Petric, R., Wolbers, M., Nguyen, C.T., Simmons, C.P., 2013. A randomized, double-blind placebo controlled trial of balapiravir, a polymerase inhibitor, in adult dengue patients. J. Infect. Dis. 207, 1442–1450.
Niyomrattanakit, P., Chen, Y.-L., Dong, H., Yin, Z., Qing, M., Glickman, J.F., Lin, K., Mueller, D., Voshol, H., Lim, J.Y.H., Nilar, S., Keller, T.H., Shi, P.-Y., 2010. Inhibition of dengue virus polymerase by blocking of the RNA tunnel. J. Virol. 84, 5678–5686.
Noble, C.G., Lim, S.P., Chen, Y.-L., Liew, C.W., Yap, L., Lescar, J., Shi, P.-Y., 2013. Conformational flexibility of the dengue virus RNA-dependent RNA polymerase revealed by a complex with an inhibitor. J. Virol. 87, 5291–5295.
Oh, J.W., Ito, T., Lai, M.M., 1999. A recombinant hepatitis C virus RNA-dependent RNA polymerase capable of copying the full-length viral RNA. J. Virol. 73, 7694–7702.
Ollis, D.L., Kline, C., Steitz, T.A., 1985. Domain of *E. coli* DNA polymerase I showing sequence homology to T7 DNA polymerase. Nature 313, 818–819.
Pawlotsky, J.-M., 2013. Treatment of chronic hepatitis C: current and future. Curr. Top. Microbiol. Immunol. 369, 321–342.
Rohayem, J., Robel, I., Jäger, K., Scheffler, U., Rudolph, W., 2006. Protein-primed and de novo initiation of RNA synthesis by norovirus 3Dpol. J. Virol. 80, 7060–7069.
Romero-Brey, I., Merz, A., Chiramel, A., Lee, J.-Y., Chlanda, P., Haselman, U., Santarella-Mellwig, R., Habermann, A., Hoppe, S., Kallis, S., Walther, P., Antony, C., Krijnse-Locker, J., Bartenschlager, R., 2012. Three-dimensional architecture and biogenesis of membrane structures associated with hepatitis C virus replication. PLoS Pathog. 8, e1003056.
Sabchareon, A., Wallace, D., Sirivichayakul, C., Limkittikul, K., Chanthavanich, P., Suvannadabba, S., Jiwariyavej, V., Dulyachai, W., Pengsaa, K., Wartel, T.A., Moureau, A., Saville, M., Bouckenooghe, A., Viviani, S., Tornieporth, N.G., Lang, J., 2012. Protective efficacy of the recombinant, live-attenuated, CYD tetravalent dengue vaccine in Thai schoolchildren: a randomised, controlled phase 2b trial. Lancet 380, 1559–1567.
Schmitt, M., Scrima, N., Radujkovic, D., Caillet-Saguy, C., Simister, P.C., Friebe, P., Wicht, O., Klein, R., Bartenschlager, R., Lohmann, V., Bressanelli, S., 2011. A comprehensive structure-function comparison of hepatitis C virus strain JFH1 and J6 polymerases reveals a key residue stimulating replication in cell culture across genotypes. J. Virol. 85, 2565–2581.
Scrima, N., Caillet-Saguy, C., Ventura, M., Harrus, D., Astier-Gin, T., Bressanelli, S., 2012. Two crucial early steps in RNA synthesis by the hepatitis C virus polymerase involve a dual role of residue 405. J. Virol. 86, 7107–7117.
Selisko, B., Potisopon, S., Agred, R., Priet, S., Varlet, I., Thillier, Y., Sallamand, C., Debart, F., Vasseur, J.-J., Canard, B., 2012. Molecular basis for nucleotide conservation at the ends of the dengue virus genome. PLoS Pathog. 8, e1002912.
Simister, P., Schmitt, M., Geitmann, M., Wicht, O., Danielson, U.H., Klein, R., Bressanelli, S., Lohmann, V., 2009. Structural and functional analysis of hepatitis C virus strain JFH1 polymerase. J. Virol. 83, 11926–11939.
Steitz, T.A., 1998. A mechanism for all polymerases. Nature 391, 231–232.
Steitz, T.A., 2006. Visualizing polynucleotide polymerase machines at work. EMBO J. 25, 3458–3468.
Tao, Y., Farsetta, D.L., Nibert, M.L., Harrison, S.C., 2002. RNA synthesis in a cage – structural studies of reovirus polymerase lambda3. Cell 111, 733–745.
Van der Schaar, H.M., Rust, M.J., Chen, C., van der Ende-Metselaar, H., Wilschut, J., Zhuang, X., Smit, J.M., 2008. Dissecting the cell entry pathway of dengue virus by single-particle tracking in living cells. PLoS Pathog. 4, e1000244.
Vignuzzi, M., Stone, J.K., Arnold, J.J., Cameron, C.E., Andino, R., 2006. Quasispecies diversity determines pathogenesis through cooperative interactions in a viral population. Nature 439, 344–348.
Vignuzzi, M., Wendt, E., Andino, R., 2008. Engineering attenuated virus vaccines by controlling replication fidelity. Nat. Med. 14, 154–161.
Welsch, S., Miller, S., Romero-Brey, I., Merz, A., Bleck, C.K.E., Walther, P., Fuller, S.D., Antony, C., Krijnse-Locker, J., Bartenschlager, R., 2009. Composition and three-dimensional architecture of the dengue virus replication and assembly sites. Cell Host Microbe 5, 365–375.
Westaway, E.G., Mackenzie, J.M., Kenney, M.T., Jones, M.K., Khromykh, A.A., 1997. Ultrastructure of Kunjin virus-infected cells: colocalization of NS1 and NS3 with double-stranded RNA, and of NS2B with NS3, in virus-induced membrane structures. J. Virol. 71, 6650–6661.
Yang, S., Chen, F.-E., De Clercq, E., 2012. Dihydro-alkoxyl-benzyl-oxopyrimidine derivatives (DABOs) as non-nucleoside reverse transcriptase inhibitors: an update review (2001–2011). Curr. Med. Chem. 19, 152–162.
Yap, T.L., Xu, T., Chen, Y.-L., Malet, H., Egloff, M.-P., Canard, B., Vasudevan, S.G., Lescar, J., 2007. Crystal structure of the dengue virus RNA-dependent RNA polymerase catalytic domain at 1.85-angstrom resolution. J. Virol. 81, 4753–4765.
Yap, L.J., Luo, D., Chung, K.Y., Lim, S.P., Bodenreider, C., Noble, C., Shi, P.-Y., Lescar, J., 2010. Crystal structure of the dengue virus methyltransferase bound to a 5′-capped octameric RNA. PLoS One 5.
Yin, Z., Chen, Y.-L., Schul, W., Wang, Q.-Y., Gu, F., Duraiswamy, J., Kondreddi, R.R., Niyomrattanakit, P., Lakshminarayana, S.B., Goh, A., Xu, H.Y., Liu, W., Liu, B., Lim, J.Y.H., Ng, C.Y., Qing, M., Lim, C.C., Yip, A., Wang, G., Chan, W.L., Tan, H.P., Lin, K., Zhang, B., Zou, G., Bernard, K.A., Garrett, C., Beltz, K., Dong, M., Weaver, M., He, H., Pichota, A., Dartois, V., Keller, T.H., Shi, P.-Y., 2009. An adenosine nucleoside inhibitor of dengue virus. Proc. Natl. Acad. Sci. U.S.A. 106, 20435–20439.
Zamyatkin, D.F., Parra, F., Alonso, J.M.M., Harki, D.A., Peterson, B.R., Grochulski, P., Ng, K.K.-S., 2008. Structural insights into mechanisms of catalysis and inhibition in Norwalk virus polymerase. J. Biol. Chem. 283, 7705–7712.
Zou, G., Chen, Y.-L., Dong, H., Lim, C.C., Yap, L.J., Yau, Y.H., Shochat, S.G., Lescar, J., Shi, P.-Y., 2011. Functional analysis of two cavities in flavivirus NS5 polymerase. J. Biol. Chem. 286, 14362–14372.